

## Properties of ceramic fabricated of synthetic carbon and organoclay based on carbon particle size

Agus Edy Pramono<sup>a,\*</sup>, R. Sugeng Mulyono<sup>a</sup>, R. Grenny Sudarmawan<sup>a</sup>, Muhammad Zaki Nura<sup>a</sup>, Haolia Rahman<sup>a</sup> and Nanik Indayaningsih<sup>b</sup>

<sup>a</sup>Department of Mechanical Engineering, Politeknik Negeri Jakarta, Jln. Prof. Dr. G.A. Siwabessy, Kampus UI. Depok 16425, Jawa-Barat, Indonesia

<sup>b</sup>Research Centre for Physics, Indonesian Institute of Sciences, Kawasan Puspiptek, Gd. 440-442, Tangerang Selatan, Banten 15310, Indonesia

The electrical and thermal conductivity properties of ceramics fabricated from carbon powder and clay have been studied. This study was designed by varying the particle size of carbon powders of mesh 150; 200; 250; 300; 350, with a carbon-organoclay ratio of 30: 70% by weight, 200 bar compacting, and sintering of 950; 1000; 1050 °C. Electrical conductivity, thermal conductivity, specific wear rate, density/porosity, and ceramic morphology have been studied. The thermal conductivity follows the tendency of electrical conductivity, because of the effect of carbon particle size. Increased sintering temperatures tend to decrease wear resistance. The smaller the particle size of carbon powder, it tends to increase the wear rate and the density of carbon-ceramic experiences relatively small changes. Porosity tends to follow density, even though the size of carbon particles gets smaller. The occurrence of porous and cracking is more due to the irregular shape of carbon and matrix particles.

**Keywords:** electrical conductivity, thermal conductivity, carbon-ceramic, carbon particle size, organoclay.

### Introduction

This study has succeeded in fabricating carbon-ceramic from coconut coir organic waste materials as electrically conductive carbon synthetic which is distributed in the organoclay as a ceramic matrix. Organoclay is a ceramic matrix that is a local material from Plered, Purwakarta, West Java, Indonesia. Synthetic carbon is produced from organic coir coconut waste carbonized at high temperatures (900 °C), producing the carbon which is electrically conductive. The electrical conductivity properties, mechanical properties of wear rate, physical properties of density and porosity, thermal conductivity properties, and morphology of carbon-ceramic composites have been studied. The relationship between these properties has been analyzed and studied. The need for friction mechanical parts that are resistant to wear and are electrically conductive is the solution that will be offered from the results of the study. The objectives of the research are development of alternative types of electrically conductive of carbon-ceramic, developing geometric alternatives and dimensions of conductor carbon particles for electrically conductive ceramics, developing techniques and engineering pro-

cesses for carbon-ceramic materials based on coconut coir waste and clay, increasing the technological value of organic waste coconut fiber, and clay, which are local ingredients. For decades, other researchers have carried out research on ceramic that is electrically conductive. Clay is an important component in making ceramic mixtures, because of its plasticity, ease of use, strength and final properties obtained by heat treatment [1, 2]. As a study conducted in 2015, developing carbon black material from agricultural waste using the pyrolysis method at varied carbonization temperatures and used as an amplifier in polymer composites [3]. The design of activated carbon-clay composites for waste decontamination made from clay and carbon has been carried out. Fluesorb B was chosen as activated carbon while a-sepiolite is a magnesium silicate clay used as an agglomerator to achieve rheological characteristics when mixed with activated carbon and water to confirm ingredients in a monolithic, solid or tubular form [4]. Research on the engineering of the use of coconut fiber into carbon-ceramic composites with electrically conductive properties has been carried out. This research was carried out experimentally based on coconut fiber with an organoclay matrix. The properties of electrical conductivity, thermal conductivity, and physical properties have been studied. This study focuses on engineering carbon-ceramic composites with a clay matrix [5]. New engineering, biochar with clay particles implanted on the surface of carbon in the biochar pore

\*Corresponding author:  
Tel : +62 811 829 833 or +62 217863530  
Fax: +62 217863530  
E-mail: agus.edypramono@mesin.pnj.ac.id

has been successfully developed [6]. The conductive aggregate type is prepared by calcining a ceramic matrix and dispersed graphite powder. The conductive aggregate prepared was used in a mortar containing carbon fiber, and the electrical resistivity and piezoresistivity of the specimen were studied [7]. Poly nanocomposites ( $\epsilon$ -caprolactone) (PCL) with carbon nanotube particles supported by clay loam (Clay-CNT) in concentration by weight were made by mixing melt. The mechanical, structural and thermal properties of nanocomposites are studied [8]. The 2015 study was to compare the fatigue behavior and oxidation resistance of CC composites (carbon) derived from metals with CC/ceramic composites (carbon/ceramics) obtained by impregnation of CC composites with polysiloxane-based preceramic and subsequent heat treatment [9]. This paper evaluates the effect of carbon nanotubes on the mechanical properties and flame resistance of Homra / OPC blends; Homra is a solid waste produced from the clay brick industry in Egypt [10]. Semi-finished ceramic composites are consolidated with various starches and sintered at different temperatures in the argon atmosphere. Electrical measurements, carbon content and Raman analysis of carbon structures determine the optimal sintering temperature of 1700 °C, which causes the formation of a uniform conductive graphite network. This carbon network produces porous composites that have high electrical conductivity, which depends on the type of starch and porous properties [11]. The composition of the ceramic material is prepared by inserting up to 20 wt % of waste into two types of clay. The raw materials used in this work are (a) one type of steel-making electric furnace waste to be combined, and (b) two types of clay that significantly differs as a matrix. The raw material is characterized by mineralogical composition, chemical composition, and particle size distribution [12]. Carbon fiber with hydrophilic surface modification is added to the mortar cement through ultrasonic treatment. The mechanical and electrical properties of carbon fiber cement mortar cement were tested to test the carbon fiber strengthening effect [13]. A new ceramic of structured hybrids of nanocarbon formed from organoclays during pyrolysis has been fabricated. It functions as a reinforcement filler and binder for carbon/carbon (C/C) composites. The heat pressing on the organoclay itself forms black monolithic sheets with high thermal stability [14]. The nature of wear resistance and electrical conductivity fabricated from the dispersion of coconut coir waste powder in the organoclay matrix have been investigated [15], the study does not consider carbon particle size as an

electrically conductive filler. The study is oriented mainly to the electrically conductive properties, the composite wear resistance properties, the physical properties of density and porosity, and composite elements. Carbon powder from coconut fibers mixed with organoclay clay, with variations in composition 10:90, 20:80, and 30: 70% by weight. Composite molds are carried out by hydraulic machines in tablet form [16]. Research on the use of sludge wastewater from industrial uniform laundry as raw material combined with kaolin clay for the production of white ceramics and the development of composites and laboratory-level sustainable technology to produce white ceramics has been carried out [17]. Based on studies of research on carbon-ceramic composites that have been carried out by many other researchers, there has been no research on carbon-ceramic composites with measurable powders, from electrical conductivity carbon of coconut coir waste, and organoclay as a matrix for ceramics with electrically conductive and wear-resistant properties. State of the art of the research are: Utilization of coconut fiber waste fiber as synthetic carbon material; The use of organoclay clay as a matrix material of carbon-ceramic; Engineering of ceramic based on waste materials and local materials for wear-resistant and electrically conductive materials; The repyrolysis sintering process is a high-temperature combustion process to obtain two ceramic characters, simultaneously in one process, electrically conductive and wear-resistant. The process of sintering to form organoclay into ceramics, while the repyrolysis process to form carbon becomes electrically conductive. The pyrolysis is a repyrolysis process, because the filler is already in the form of synthetic carbon from organic waste; The repyrolysis sintering process is carried out in a tightly closed reactor tube, without inert gas (nitrogen or argon). The two-process experiments also contributed to the technology of carbon-ceramic fabrication processes.

## Experiments

### Material preparation

Organoclay is a local material as a ceramic matrix. Synthetic carbon powder is carbonized at 900 °C from organic coir coconut waste. Organoclay elements were examined by an X-ray Fluorescence Analyzer TORONTECH TT - EDXPRT, the main element of the organoclay was silica (51.4%), the same thing was done by other researchers with silica element (an average of 50.5%) [18], 61.1% SiO<sub>2</sub> element [19]. The results of testing the organoclay elements are shown in

**Table 1.** Elements of organoclay

Elements	Si	Fe	Al	Ti	Mn	Cr	Zr	Sb	Sn	Cu	Ni	Ga	Zn	Total
% weight	51.4	28.1	16.1	2.41	1.13	0.33	0.22	0.2	0.1	0.03	0.03	0.01	0.01	100.07
± %	2	2.2	0.9	0.15	0.11	0.12	0.01	0.3	0.13	0.01	0.02	0	0	

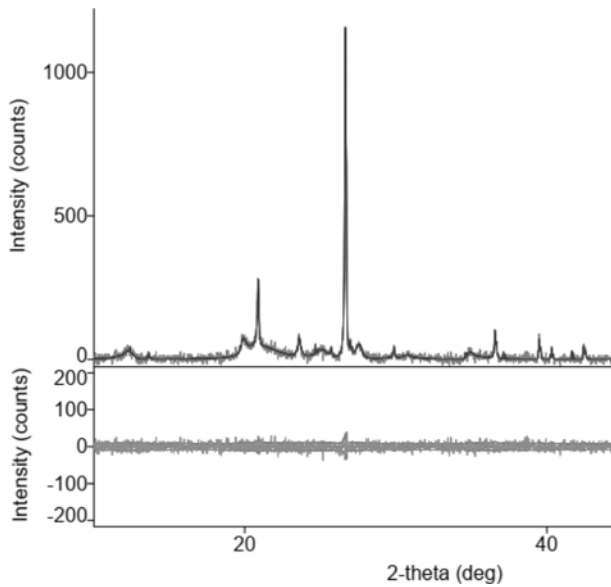


Fig. 1. X-Ray Diffractions of organoclay.

Table 1.

Fig. 1 shows the X-ray diffraction of the organoclay, at an angle of 2 thetas, between 20-30°, the position of the highest peak of intensity (> 1000), showing the silica element contained in the organoclay. The same characteristic graph of clay was also shown by other studies, [20, 15, 16, 21-23].

**Fabrication of specimens**

The coconut coir pyrolysis process is carried out in a furnace with an airtight tube. Milling is conducted with a crusher to reach a mesh size of 150; 200; 250; 300; 350, was sieved with a sieve vibrator. Mixing carbon powder with organoclays for the formation of mixed plasticity, with a composition ratio of carbon powder and clay mixture designed 30:70, produced 30 green compact specimens. Compaction was carried out with a hydraulic press machine with a pressure of 200 bar, resulting in a green compact tablet with a size of 40 mm in diameter × 10 mm thick. Repyrolysis sintering was carried out in a furnace with an airtight reactor tube, at temperatures varying from 950; 1000; 1050 °C, with a temperature velocity of 2 °C/min, carbon-ceramic is produced with electrically conductive properties. The total specimens are shown in Table 2.

**Electrical conductivity test**

Electrical conductive properties were tested using the two-point probe method, with a modification of the copper plate electrode instead of the probe. Measurements were made against the DC electric current resistance using a digital multimeter, specimen diameter, and thickness of carbon-ceramic specimens. The measurement of electrical conductivity follows the ASTM D257 standard [15, 16, 5, 24, 25]. The testing method is shown in Fig. 2.

Table 2. Number of specimens

Sintering temperature °C	The size of the carbon particle, mesh					Total
	150	200	250	300	350	
950	10	10	10	10	10	50
1000	10	10	10	10	10	50
1050	10	10	10	10	10	50
Total						150

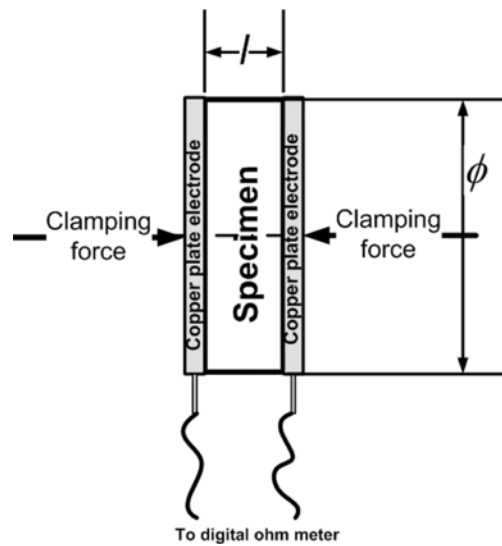


Fig. 2. Two plate electrodes testing method.

Measurements were made of electrical resistance, specimen thickness, and cross-sectional area of specimens for electricity. Electrical static resistance is calculated by the equation,

$$\rho = \frac{R \times A}{l} \tag{1}$$

The amount of electrical conductivity is determined by the equation,

$$\sigma = \frac{1}{\rho} \tag{2}$$

Note:  $\rho$  = static electricity resistance [ $\Omega\text{m}$ ];  $R$  = electrical resistance [ $\Omega$ ];  $A$  = cross-sectional area of specimens [ $\text{m}^2$ ];  $l$  = length of current path [ $\text{m}$ ];  $\sigma$  = electrical conductivity of specimens [ $1/\Omega\text{m}$ ] or [ $\text{S/m}$ ].

**Thermal Conductivity test**

Testing of thermal conductivity to determine thermal physical properties, especially heat conductivity, of carbon-ceramic to heat flow. This test refers to the ASTM E1530 standard for evaluating resistance to thermal transmission of materials through the protected heat flow meter technique [5]. This test method includes a steady-state technique in determining resistance to thermal transmission. Two solid samples were prepared with a diameter of 50 mm and a thickness of 4 mm and 2 mm from each sample.

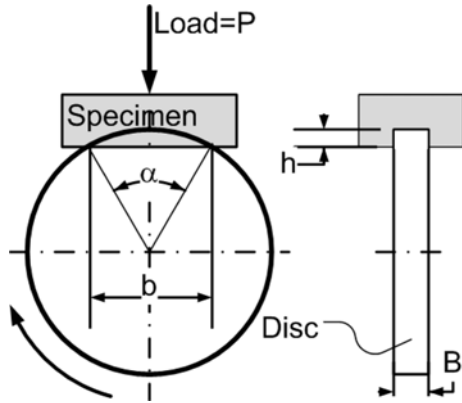


Fig. 3. Disc-wear testing method.

$$k = \frac{l_b - l_a}{l_b/k_b - l_d/k_a} \quad (3)$$

Note:  $l$  and  $k$  refer to the thickness of the sample and thermal conductivity respectively. Subscripts  $a$  and  $b$  show two different sample thicknesses.

**Wear resistance test**

Wear rate testing is carried out to determine the resistance of carbon-ceramic to friction using a disc wear tester. Different studies use the wear resistance test method with the ball-on-disk method [26].

Another study uses the pin-on-disk method, to test the wear rate [27, 28]. In this study, wear rate testing follows ASTM C1243-93 (2015) standards [29, 30], with a disc-wear testing machine. Shown in Fig. 3. The specific wear rate is calculated by the equation,

$$w_{rate} = \frac{B}{L \times P} \left[ \frac{\pi \times r^2}{180} \arcsin\left(\frac{b}{2.r}\right) - \frac{1}{2} \times b(r-h) \right] \quad (3)$$

Note:  $W_{rate}$  = specific wear rate [mm<sup>3</sup>/Nm];  $b$  = trace length [mm];  $L$  = distance [m];  $P$  = test load [N];  $r$  = disk radius [mm];  $B$  = trace width [mm];  $h$  = trace depth [mm].

**Density test**

A density test is conducted to determine the density level of carbon-ceramic. Another study determined the density by weighing the specimen weights then divided by the volume of the specimen [14]. This study, the density test was conducted experimentally using the Archimedes method based on the ASTM D792 standard [16, 31, 32, 11, 33, 34, 35]. The density of carbon-ceramic is calculated by the equation,

$$\rho_{carbon\ ceramic\ composite} = \frac{W_A}{W_B - W_C} \times \rho_{Distilled\ water} \quad (4)$$

**Porosity test**

The porosity test is to determine the percentage of voids and voids contained in the carbon-ceramic volume. The porosity test applies the Archimedes method

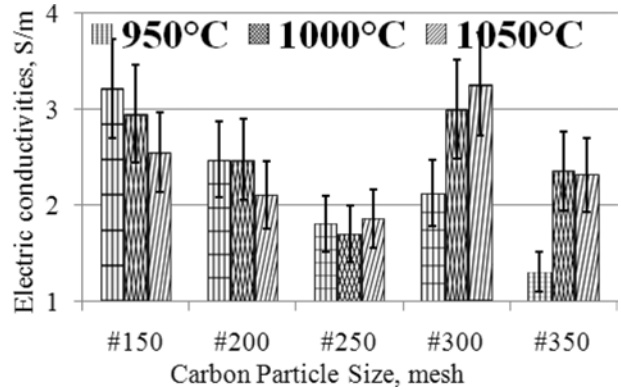


Fig. 4. The relationship of electric conductivities vs. carbon particle size vs. sintering temperature.

following the ASTM C20 - 00 (2015) standards [16, 11 33, 36, 37]. Porosity is calculated as follows,

$$P = \left( \frac{W_B - W_A}{W_C} \right) \times 100\% \quad (5)$$

Note:  $W_A$  = dry weight [gram];  $W_B$  = saturated weight of water in the air [gram];  $W_C$  = saturated weight of water in the water [gram];  $\rho_{composite}$  = composite density [g/cm<sup>3</sup>];  $\rho_{distilled\ water}$  = the density of distilled water 0.992 [g/cm<sup>3</sup>]

**Morphological tests**

This test was conducted to determine the morphological conditions of carbon-ceramic on a micro-scale. Based on the morphology of carbon-ceramic, the geometric shape of the particles can be identified, both matrix and carbon particles, the interface bond between the particles can be known, and the appearance of cavities that cause porosity of the ceramic can be identified. Morphological tests were conducted with Hitachi SU 3500 microscopic scanning electron.

**Result and Discussion**

**Electrical conductivity**

The purpose of measuring electrical conductivity is to determine the highest electrical conductivity value of carbon-ceramic. Electrical conductivity values are arranged in graphical form, as shown in Fig. 4.

The highest electrical conductivity was produced by specimens with carbon particle size #300, with a sintering temperature of 1050 °C, an electrical conductivity value of 3.26 [S/m]. Meanwhile, the lowest 1.31 [S/m] is produced by specimens with carbon particle size #350 at a sintering temperature of 950 °C. The condition of the specimen with carbon particle size # 150, when the sintering temperature increases, the electrical conductivity decreases, also experienced by carbon-ceramic with particle # 200, whereas for samples with carbon particle # 250, the electrical conductivity produced is

relatively constant. Specimens with particle sizes #300 and #350, when the sintering temperature is increased it tends to increase the electrical conductivity of the specimens. In general, at mesh particle size # 150; 200; 250, the electrical conductivity decreases further, when the sintering temperature is raised, from 950 °C to 1050 °C. In specimens with mesh particle sizes # 300 and # 350, and higher sintering temperatures (from 950 °C - 1050 °C), this will increase electrical conductivity. Factors affecting DC conductivity in solids are current carrier concentration, temperature, defective density and/or structural irregularities, and facilities where ions can jump to adjacent empty locations [38, 2]. The particles in this study are small carbon which is homogeneously dispersed which acts as a conductive phase in the ceramic matrix [24]. The more carbon particles as a conductor filler, and cling tightly to the ceramic matrix will result in good interface contact, and this will increase the electrical conductivity the better. When the carbon content is at the percolation limit, a continuous electrically conductive path begins to form, that is, an electric current can flow between adjacent carbon particles through direct contact or tunneling effects, and so the resistance decreases. The conductor filler network is formed by the relationship between the conductor fillers that are close together and stick together. Based on the volume fraction of few-layer graphene in multilayer composites, it produces electrical conductivity from  $1 \times 10^{-14}$  to  $1 \times 10^{-4}$  [S/cm] [25]. Engineering ceramics from clay illite, the results of AC electrical conductivity tests show values from  $1 \times 10^{-2}$  to  $1 \times 10^{-7}$  [S/m] [2]. The electrical properties of the insulant appear to be very dependent on the chemical and mineralogical composition of the clay used, and the soaking period used. The study of the use of clay from Indian Jammu, for insulant ceramics, produces electrical conductivity of around  $0.5$  to  $2 \times 10^{-8}$  [mhos/cm] [39]. The electrical properties of aluminum nitride ceramics show electrical resistance from  $1 \times 10^{10}$  to  $1 \times 10^{14}$  [ $\Omega$  cm] [40].

### Thermal conductivity

Testing of thermal conductivity to determine thermal physical properties, especially heat conductivity, of carbon-ceramic to heat flow. Thermal conductivity testing has also been carried out in other studies, with different methods, [41, 42, 43, 44, 45]. The highest thermal conductivity is  $\pm 0.45$  [W/m°C], produced from specimens with carbon particle size # 250, in the sintering process of 1050 °C. The lowest thermal conductivity is  $\pm 0.1$  [W/m°C], produced from carbon-ceramic with particle # 350, at sintering temperatures of 1000 °C. This is shown in Fig. 5, the deviation values of each sample variant are shown, with an average deviation value not higher than 10%.

The smaller the particle size of carbon, the smaller the thermal conductivity produced by carbon-ceramic.

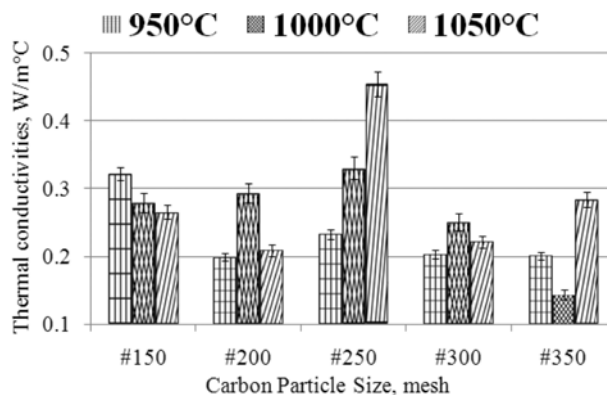


**Fig. 5.** The relationship of thermal conductivity vs. carbon particle size vs. sintering temperature.

This occurs at sintering temperatures of 950 °C and 1000 °C. Meanwhile, at a sintering temperature of 1050 °C, indicating that the smaller the particle size, the increase in thermal conductivity. The effect of sintering temperature on the thermal conductivity of carbon-ceramic also shows an unequal tendency. As shown in Fig. 5, the mesh size # 150 shows that the higher the sintering temperature, the lower the thermal conductivity. Meanwhile, samples with mesh # 200 to mesh # 350 show increased thermal conductivity, when the sintering temperature is increased from 950 to 1050 °C. In comparison, other studies have also produced thermal conductivity, which is shown as follows. Allegreta studied the thermal conductivity values of kaolin samples with kaolinitic clay (kaolinite = 58%, illite = 18%, smectite = 2%, quartz = 22%, rutile and anatase in the trace). The highest thermal conductivity value is  $\pm 0.68$  [W/mK] produced by kaolin samples with tempering temperatures up to 1000 °C, and the lowest is  $\pm 0.28$  [W/mK] [46]. The raw material used in this study is kaolin powder which is marketed by the company Denain-Anzin-Minéraux (France). When the temperature increases, the sintering process implies better material consolidation due to the decomposition of clay particles in the mullite phase and amorphous flux which is rich in silica. This study produced a thermal conductivity of 0.28 to 0.63 [W/mK] [47]. The clay-based ceramics investigated in this study were made of clay, sand, and water. Clay is extracted as a batch in a clay mine to ensure homogeneity. Clay-based ceramics produce thermal conductivity of 1.07 [W/mK] [43]. Three commercially available soil-based plasters, widely used for interior wall base systems in several European countries, selected for experimental testing. The thermal conductivity of the sample disk made from the soil plaster material examined is measured. This study yields thermal conductivity of 0.74 to 1.16 [W/mK] [48]. The clay material supplied by Ceradel company (Saint Amand en Puisaye, France) is a mixture of extruded clay that is used for making pots. To ensure good homogeneity, the raw material is first mixed in water.

This study yields thermal conductivity of  $\pm 0.4$  to  $1.8$  [W/mK] [49]. Clay-based materials which exhibit high pore volume fractions and low thermal conductivity suitable for thermal insulation have been studied. This study shows a thermal conductivity of  $0.063$  to  $0.130$  [W/mK] [44].

### Specific wear rate

Wear rate testing is performed with a disc wear tester, by measuring the variables of wear depth, wear trail length, wear trail width, load, rotational speed, distance traveled. The lowest wear rate is produced by carbon-ceramic with carbon particle size # 200, at a sintering temperature of  $1000$  °C, which is  $3.59827 \times 10^{-5}$  [mm<sup>3</sup>/Nm], in this condition this material shows the highest hardness compared to other specimens, of the size different carbon particles. The softest specimens in this study produced the highest wear rate,  $0.000752239$  [mm<sup>3</sup>/Nm], this was demonstrated by specimens with carbon particle size #350, at sintering temperatures of  $1050$  °C, as shown in Fig. 6. The graph shows that the higher the sintering temperature the higher the wear rate produced, the condition shows that the increase in sintering temperature tends to decrease the wear resistance properties, in other words, the softer the specimens. Carbon-ceramic tend to show relatively stable wear rates at particle size # 150, even though the sintering temperature is raised to  $1050$  °C. This specimen shows the harshest mechanical character. Likewise, the smaller the particle size of carbon powder tends to increase the wear rate, meaning that carbon-ceramic is softer, and is not resistant to mechanical friction. Wear rate is one of the mechanical properties of carbon-ceramic; this mechanical property can also represent the level of hardness of the material. Indirectly can also show the level of strength of the carbon-ceramic. The concept is, the lower the wear rate, the higher the level of hardness of the ceramic, and thus the higher the tensile strength of the specimens, with the structure of the material being isotropic. As in this study, this carbon-ceramic is designed isotropic, therefore using powder-shaped filler. The weakness of the mechanical properties of this material is thought to be caused by porous cavities formed in carbon-ceramic, although the fabrication process of carbon-ceramic tablets applies a pressure of  $200$  bars, with a hydraulic press.

Allegedly, when printing green compact, there are air cavity bubbles trapped inside, so that during the sintering process the air cavity forms porous in a carbon-ceramic. Some elements of the organoclay are thought to have also burned during the high-temperature sintering process; this will form a porous in the material. As explained in the analysis of relationships of porosity and composite wear rates. This study tested the wear rate using the two-body abrasive wear test method, which was carried out using a pin on disc

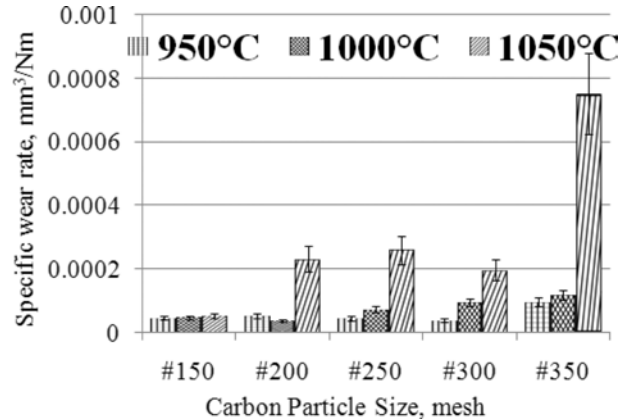


**Fig. 6.** The relationship of specific wear rate vs. carbon particle size vs. sintering temperature.

tool. This study shows the wear rate based on weight loss from the material being tested [29]. Other researchers applied specific wear rate testing to the ASTM G99-95a standard producing specific wear rates with values from  $5 \times 10^{-7}$  to  $1.5 \times 10^{-5}$  [mm<sup>3</sup>/Nm] [50]. The wear rate of the C/C-SiC composite produces a specific rate of  $2.5 \times 10^{-4}$  to  $5 \times 10^{-4}$  [mm<sup>3</sup>/Nm] [51]. The engineering of carbon-ceramic composites from other studies shows testing the wear rate based on the level of hardness of the composite [28].

### Carbon-ceramic density

Density testing is carried out to determine the level of density of carbon composites. This test was carried out experimentally using the Archimedes method based on the ASTM D792 standard [30, 34, 35, 37]. The condition of the density will indicate the degree of porosity of the specimens.

The lower the densities level of the carbon-ceramic, the higher the porosity of the specimens.

This will affect the level of electrical conductivity and ceramic wear resistance. The density of carbon-ceramic is arranged in graphical form as shown in Fig. 7. The engineering of carbon-ceramic shows the physical properties of relatively stable densities between  $1-1.2$  [gram/cm<sup>3</sup>]. In detail, it can be proven that there is an increase in density when the sintering temperature is increased, but an increase in density of about  $0.2$  [gram/cm<sup>3</sup>], when observing the deviation value, the value of increasing density is not significant. Changes in carbon particle size from #150 - #350 also do not make significant changes in densities. As shown in Fig. 7. The smaller the particle size of carbon, the density is relatively unchanged. As a comparison to the results of other studies, explained as follows. This researcher utilizes kaolin for compacting and sintering with temperature variations from  $980 - 1200$  °C, producing densities of  $2.55$  to  $2.9$  [grams/cm<sup>3</sup>], and porosity of  $6.3$  to  $35.4\%$  [47]. A study of ceramics fabricated from kaolin, bentonite, and sand. To investigate the evolution

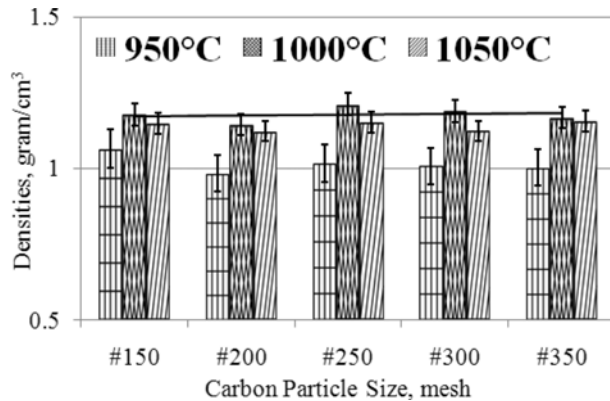


**Fig. 7.** The relationship between densities vs. carbon particle size vs. sintering temperature.

of electrical resistivity of various layers of kaolinite dominant clay, in terms of soil composition, due to moisture content and dry density changes. This research resulted in a composite density between 0.72 to 1.87 [gram/cm<sup>3</sup>] [52]. A carbon-ceramic composite fabricated from fly ash, carbon fiber, and other particles, compacted 200 [kg/cm<sup>2</sup>], heated to 1000 °C, has produced densities between 1.65 to 1.87 [gram/cm<sup>3</sup>] [28].

### Carbon-ceramic porosity

The porosity test applies the Archimedes method following the ASTM C20 - 00 (2015) standards [16, 11, 33, 37]. Carbon-ceramic shows relatively high porosity, between 33 - 42% porosity. Based on consideration of the deviation of carbon-ceramic in the 950 °C sintering process shows the percentage of porosity that is relatively stable, between 33 - 36%, even though the particle size gets smaller, from mesh # 150 - # 350, while carbon-ceramic with the same mesh particle size (# 150 - # 350) which is processed by sintering 1000 °C, producing porosity between 40 - 45%, while carbon-ceramic processed by sintering at temperatures of 1050 °C show porosity between 38 - 42%, with a mesh size change of # 150 - # 350. The porosity of carbon-ceramic is even greater when the sintering process temperature is raised from 950 - 1050 °C, with an equal composition ratio of 70: 30%, as shown in Fig. 8. This condition is thought to be due to the fact that most organoclay matrices turn to carbon when sintering is processed at high temperatures. This increases the volume of carbon in the carbon-ceramic, and carbon has a high absorption of water when testing porosity.

Broadly speaking, the smaller the size of carbon particles in carbon-ceramic, the porosity contained by carbon-ceramic is relatively stable, there is no significant change. In comparison, several researchers, using the same method, produced the porosity described below. Because the particles grow irregularly, the ability of the particles to bear the external force decreases when an external load is applied. The compressive strength of the sample is reduced due to an increase in porosity,

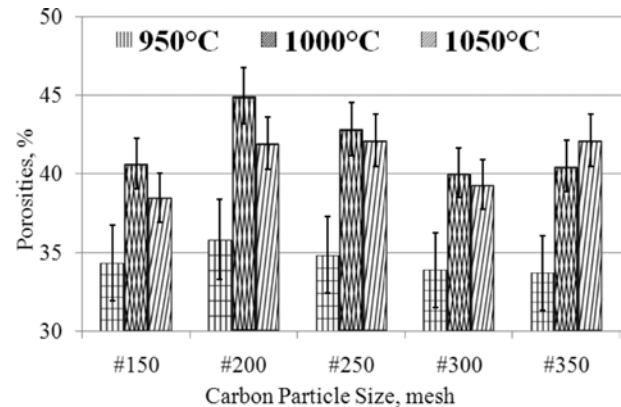


**Fig. 8.** The relationship of porosities vs. carbon particle size vs. sintering temperature.

which is caused by a pile of compressed particles between the particles, this study produces a porosity of 70 to 80% [53]. Another study showed the real porosity of the K1 and K2 specimens calculated according to the Archimedes principle, each equivalent to 21.9 and 19.9%. Thus, round silica solids show lower porosity, that is, denser microstructure [36]. This study shows the results of porosity testing of various types of ceramic specimen particle sizes and produces porosity between 14 to 43% [54]. This researcher utilizes bentonite as a mixture for clay and silica ceramics producing porosity from 10 to 50% [37].

### The relationship of density to porosity

This analysis is to show the interdependence between density and porosity. The concept which states that when density increases, porosity will decrease, does not apply significantly in the facts of this study. Figure 9 (a); 9 (b); and 9 (c) show that when the carbon particle size gets smaller the density shows a decrease, followed by a decrease in the percentage of porosity volume. This occurs relatively similarly at all sintering temperatures. Fig. 9 (a) shows the same tendency between density and porosity of carbon-ceramic composites which are processed by sintering at 950 °C.

The fact that relatively similar trends are also shown by carbon-ceramic by sintering at temperatures of 1000 °C, as shown in Fig. 9 (b), when the size of carbon particles decreases, the density also decreases and is followed by decreasing porosity. The same relative thing is also shown in Fig. 9 (c), the density increases and is followed by increased porosity as well, at the particle size reduction of mesh #150 - #350, at a sintering temperature of 1050 °C. The fact that happens is, porosity tends to follow density, even though the size of carbon particles gets smaller.

### The effect of the density to electrical conductivity

Density is a physical property that shows a specific level of material weight in units of volume, it can be

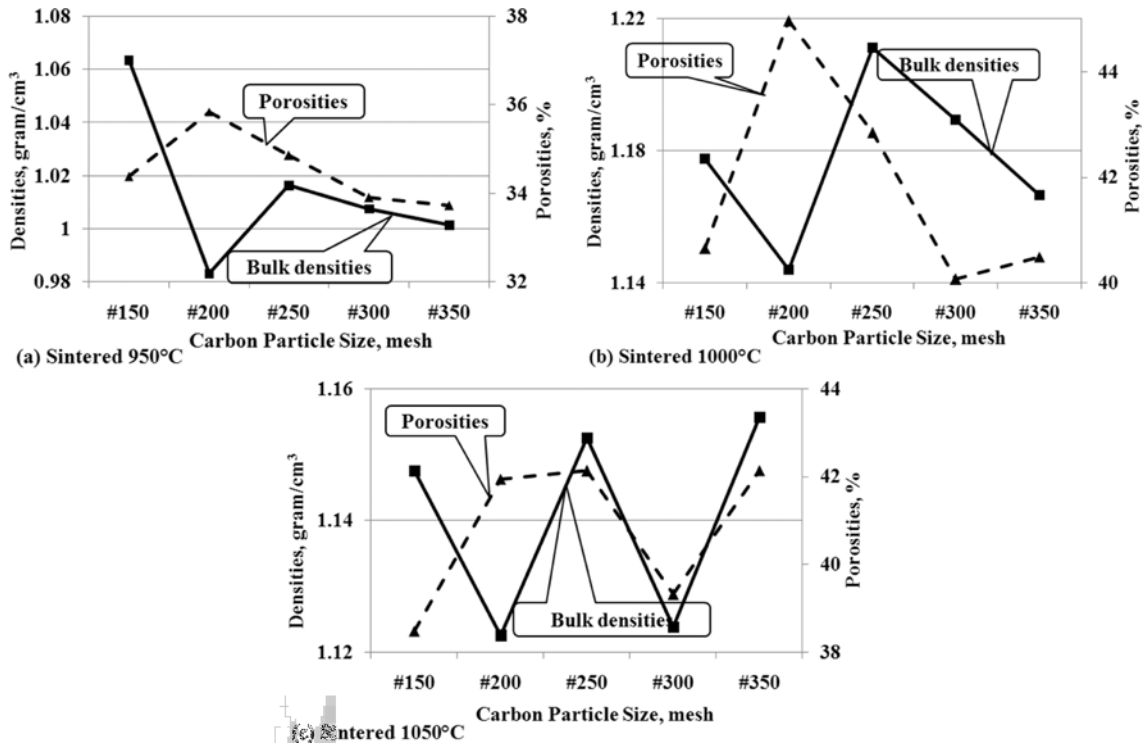


Fig. 9. The relationship between densities vs. porosities vs. carbon particle size.

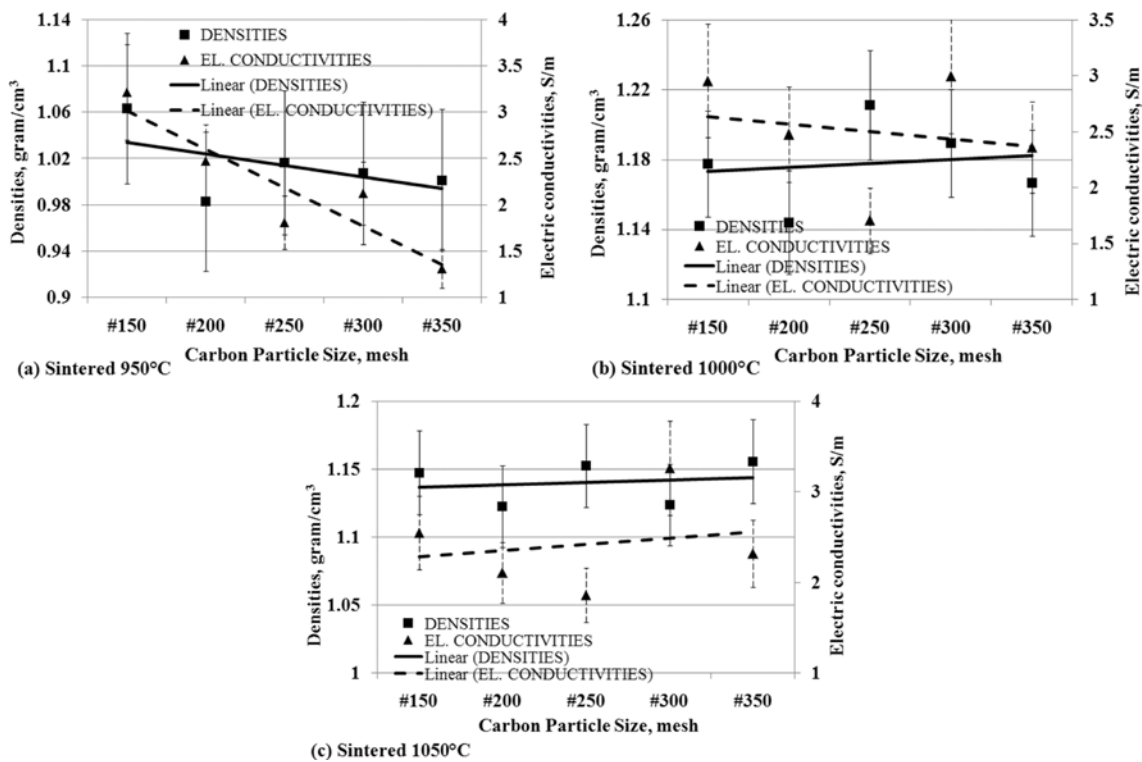


Fig. 10. The relationship between densities vs. electric conductivities vs. carbon particle size.

named density. The fact that occurs in the fabrication of carbon-ceramic shows that the density affects the electrical conductivity, as shown in Fig. 10. Fig. 10 (a) is a fact of carbon-ceramic with a sintering process at a

temperature of 950 °C, which shows the smaller particle size carbon spread in the specimens makes electrical conductivity decreases, following the decrease of the density.



Carbon-ceramic with a 1000 °C sintering process shows a different fact, the smaller the size of carbon particles, indicating an increase in the density of the carbon-ceramic, but conversely, the electrical conductivity actually decreases, as shown in Fig. 10 (b). The decrease in carbon particle size in the specimens gives an increase in the density of the carbon-ceramic and is followed by an increase in electrical conductivity shown by carbon-ceramic by sintering at temperatures of 1050 °C, as shown in Fig. 10 (c). In general, an increase or decrease in carbon-ceramic density based on carbon particle size is followed by an increase or decrease in the electrical conductivity of carbon-ceramic.

**The effect of the porosity to electrical conductivity**

The level of porosity of carbon-ceramic will affect the level of electrical conductivity.

Porosity is cavities formed in ceramic due to compaction. Cavities formed on carbon-ceramics cause connectivity between carbon conductivity particles to be disrupted and become a barrier to the flow of electricity. This study shows that the smaller the change in the particle size of carbon powders, the lower the porosity volume of carbon-ceramics followed by a decrease in electrical conductivity.

This is experienced by carbon-ceramic at sintering temperatures of 950 °C, as shown in Fig. 11 (a). Likewise, carbon-ceramic with a sintering temperature

of 1000 °C experienced the same decrease between the porosity volume and the electrical conductivity of the specimens, as shown in Fig. 11 (b). Different characteristics are shown in carbon-ceramic with sintering temperatures of 1050 °C, the smaller the particle size of carbon, the greater the percent porosity volume, and followed by an increase in electrical conductivity of carbon-ceramic. This is shown in Fig. 11 (c).

**The effect of porosity to specific wear rates**

Cavities are formed in carbon-ceramics, which weaken the mechanical bonding of filler particles and matrix particles, and between filler particles and matrices. This fact is shown in Fig. 12. Theoretically, when the percentage of porosity increases, it will form a weak bond between the particles, producing a weak bond mechanically. The greater porosity percentage indicates the number of cavity volumes in the specimen more and more, and the bond between particles is mechanically weaker, so the wear rate gets higher, or carbon-ceramic becomes softer, hardness decreases and easily wears out. Conversely, a small percentage of porosity indicates a small number of cavities in carbon-ceramics, and increases mechanical bonding between particles, both fillers, matrices, and between matrices and fillers, and thus strengthens the mechanical properties of these specimens. This research does not always show the similarity of characteristics with theoretical

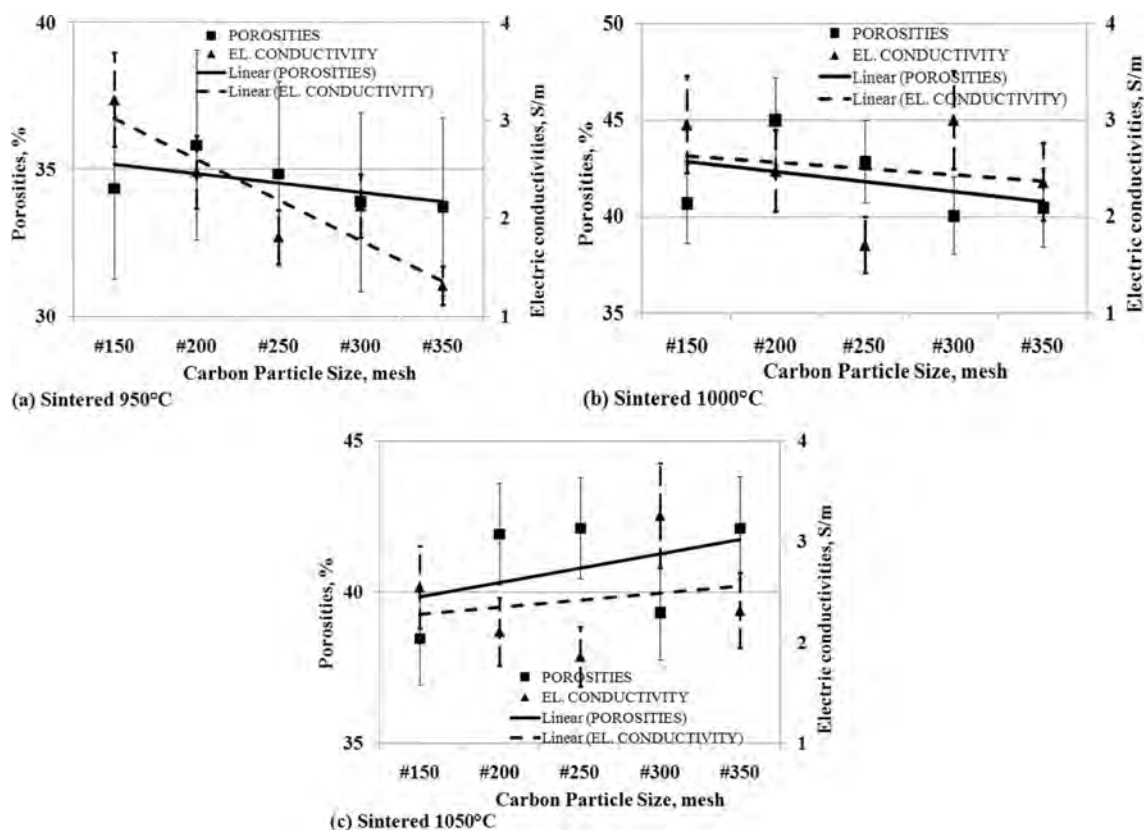
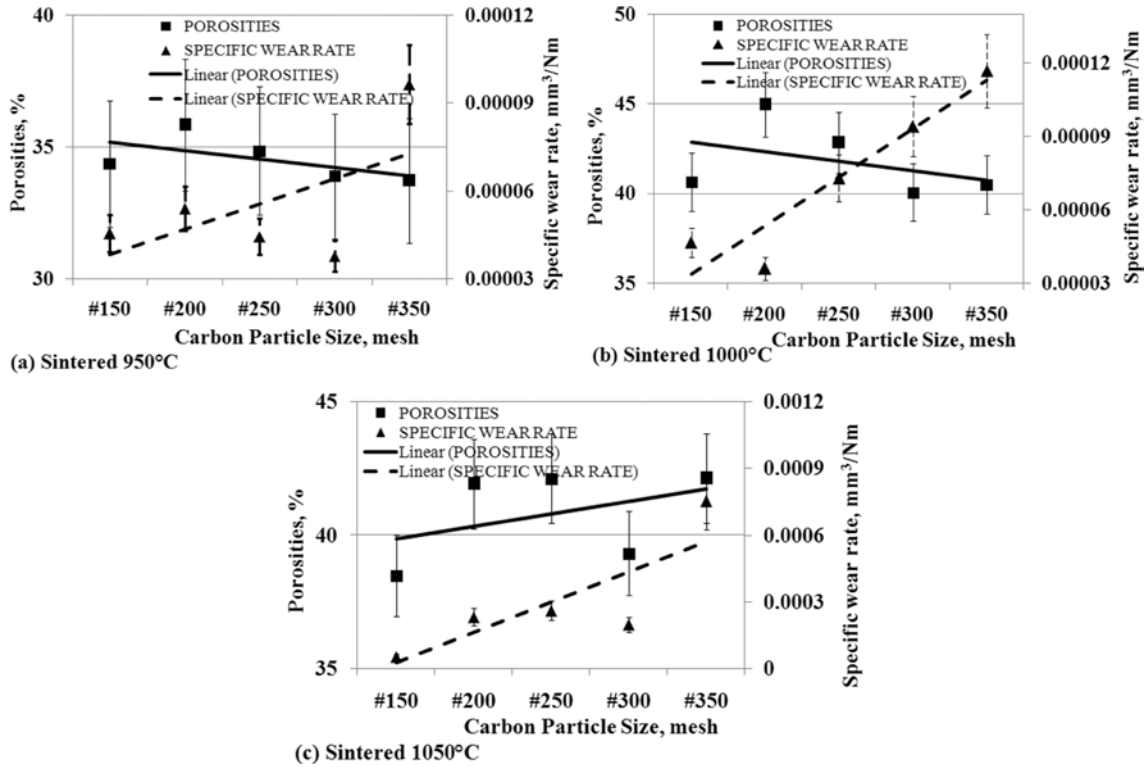


Fig. 11. The relationship of porosities vs. electric conductivities vs. carbon particle size.



**Fig. 12.** The relationship of porosity vs. specific wear rate vs. carbon particle size.

concepts. Carbon-ceramic with a sintering temperature of 950 °C shows the opposite character.

When the particle size of the carbon powder gets smaller, resulting in a smaller percentage of porosity, but vice versa is followed by an increase in higher wear rates, which means that this type of specimen exhibits weaker mechanical bonding properties, its hardness decreases, as shown in Fig. 12 (a). Likewise, the characteristics shown by carbon-ceramics by the sintering temperature process of 1000 °C, show the same character, this is shown in Fig. 12 (b). Different characters are shown by carbon-ceramic with sintering temperatures of 1050 °C, shown in Fig. 12 (c). The study shows, the smaller the particle size of carbon powders results in greater porosity percentages and is followed by the higher wear rate of the specimens. This fulfills the concept that the more cavities in the carbon-ceramic will weaken the mechanical bonding properties of the materials, and thus weaken the mechanical properties, increasing the wear rate of carbon-ceramic.

### The relationship of thermal conductivity to the electric conductivity

Thermal conductivity has a relationship with electrical conductivity. When thermal conductivity decreases, it is followed by reduced electrical conductivity.

This is shown in Fig. 13 (a) and (b), which are produced from carbon-ceramic with sintering temperatures of 950 °C and 1000 °C. The smaller the particle size of carbon, the value of thermal and electrical conductivity

decreases. Carbon-ceramic with the sintering process of 1050 °C produces different tendencies, as shown in Fig. 13 (c). The figure shows that the smaller the particle size of carbon, the more thermal and electrical conductivity increases. Based on the facts of the analysis, the tendency of thermal conductivity will be followed by the tendency of electrical conductivity.

### Morphology of carbon-ceramic

Microphotographs from the scanning electron microscopic test cannot distinguish morphology based on the ratio of composition between carbon and organoclay and also based on sintering temperature, this test will show the size of carbon particles scattered in the ceramic matrix of organoclays. The test was carried out with a Hitachi SU 3500 scanning electron microscopic testing machine. The purpose of this test is to look at the morphological state of carbon-ceramic. To see the possibility of cavity formation on the specimens and the interface bond between organoclay and carbon powder from coconut coir powder. Cavities formed in the specimens will weaken the electrical conductivity and wear resistance of the carbon-ceramic. Morphological are shown in Fig. 14 (a) to 14 (j). The shape and geometric carbon powder, in general, is elongated and irregular, and not granule or round in shape. The size of the carbon powder is shown in the elongated micron size, 90 μm, shown by carbon-ceramic with mesh size # 150, as shown in Fig. 14 (a). Based on the ASTM wire mesh standard, the 90 μm particle size is relevant

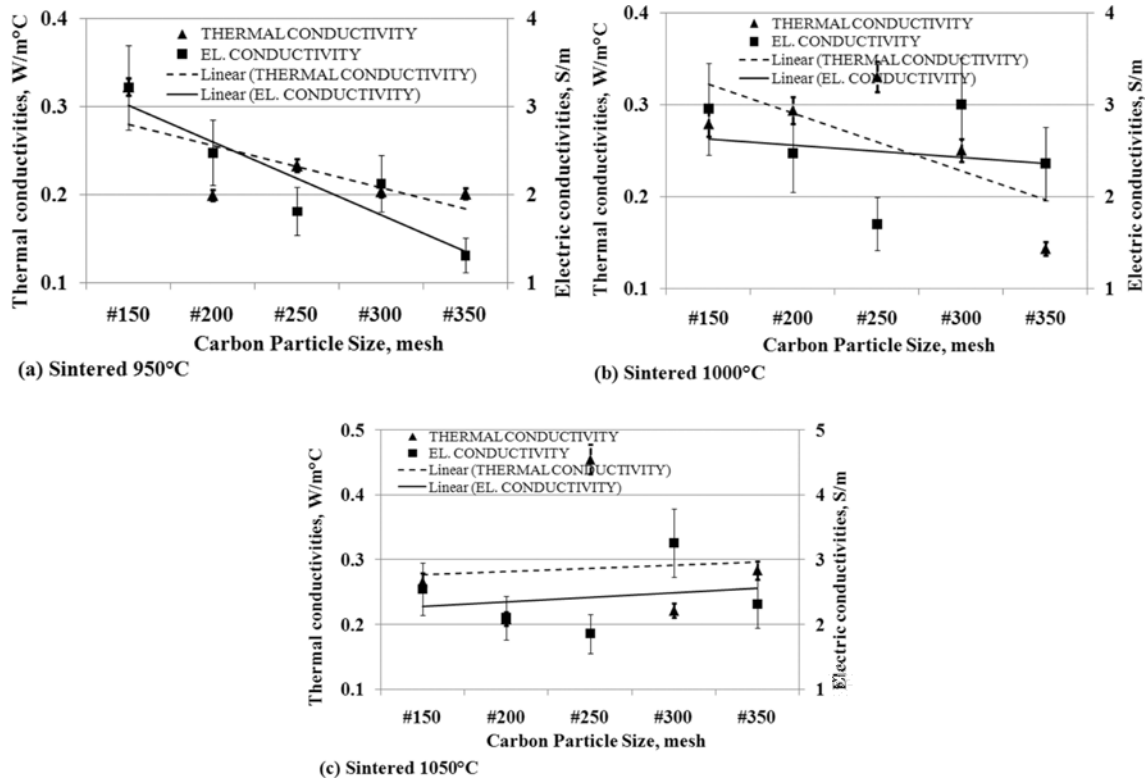


Fig. 13. The relationship of thermal conductivity vs. carbon particle size vs. electric conductivity.

to the standard mesh size number between 140 to 170. Fig. 14 (a) and (b) with magnifications of 750 and 2000 also shows the interface cracks between carbon particles against organoclay matrix particles, silica particles from organoclay matrices, mechanical bonding between particles are also shown in the carbon-ceramic morphology. The smaller carbon particle size is shown in Fig. 14 (c), the figure is the morphology of carbon-ceramic with carbon particle size # 200, with an elongated particle size of 63.5  $\mu\text{m}$  this particle size is relevant to the ASTM standard wire mesh sieve chart numbers between 200 to 230. In general, shapes and geometric carbon particles are elongated and irregular in shape, and have dark features, as shown in Fig. 14 (c) and (d), with magnifications of 750 and 2000. Also shown in the picture are silica particles from the organoclay matrix, that are shown with bright white features, cracks interface between carbon particles against the matrix, between particles of the matrix, mechanical bonding between matrix and carbon particles. Carbon-ceramic with mesh # 250 shows elongated geometric carbon particles measuring 51  $\mu\text{m}$ . This dimension is relevant to the ASTM wire mesh standard between numbers 270 to 325. At magnifications 750 and 2000, shown in Fig. 14 (e) and (f) is the morphology of the interface cracks between carbon particles against organoclay matrix particles, silica particles of the matrix, mechanical bonding between particles. The morphology of carbon-ceramic particles with mesh size # 300 is

shown in Fig. 14 (g) and (h), at magnifications of 750 and 2000. The morphology shows the irregular geometric shape of particles, both carbon particles, and organoclay matrix particles. The measurement results of carbon particles show 44  $\mu\text{m}$ , this is relevant to the ASTM standard wire mesh sieve chart between numbers 325 to 400. Interface cracks between carbon particles against the organoclay matrix are also shown in the figure. The bright white feature indicates the content of silica particles from the organoclay matrix. While the dark, irregular, and elongated black features indicate carbon particles, or it is also suspected to be very strong is the crack or porous of the specimens. The morphology of carbon-ceramic with mesh size # 350 shows the carbon particle size of 41  $\mu\text{m}$ , as shown in Fig. 14 (i). The carbon particle size is relevant to the ASTM sieve chart standard wire numbers between numbers 325 to 400. Fig. 14 (i) and 14 (j) show geometric irregular carbon particles and matrices, showing mechanical bonds between particles, showing the interface cracks between filler particles and matrices. The white and bright features in the morphology indicate the silica content of the organoclay matrix. Meanwhile, the dark morphological features indicate carbon particles and a very strong suspicion is cracks or porous that occurs within the carbon-ceramic. This study shows that compaction load of 200 bars and with smaller particle size apparently cannot eliminate porous or cracks that occur in the specimens. The strong

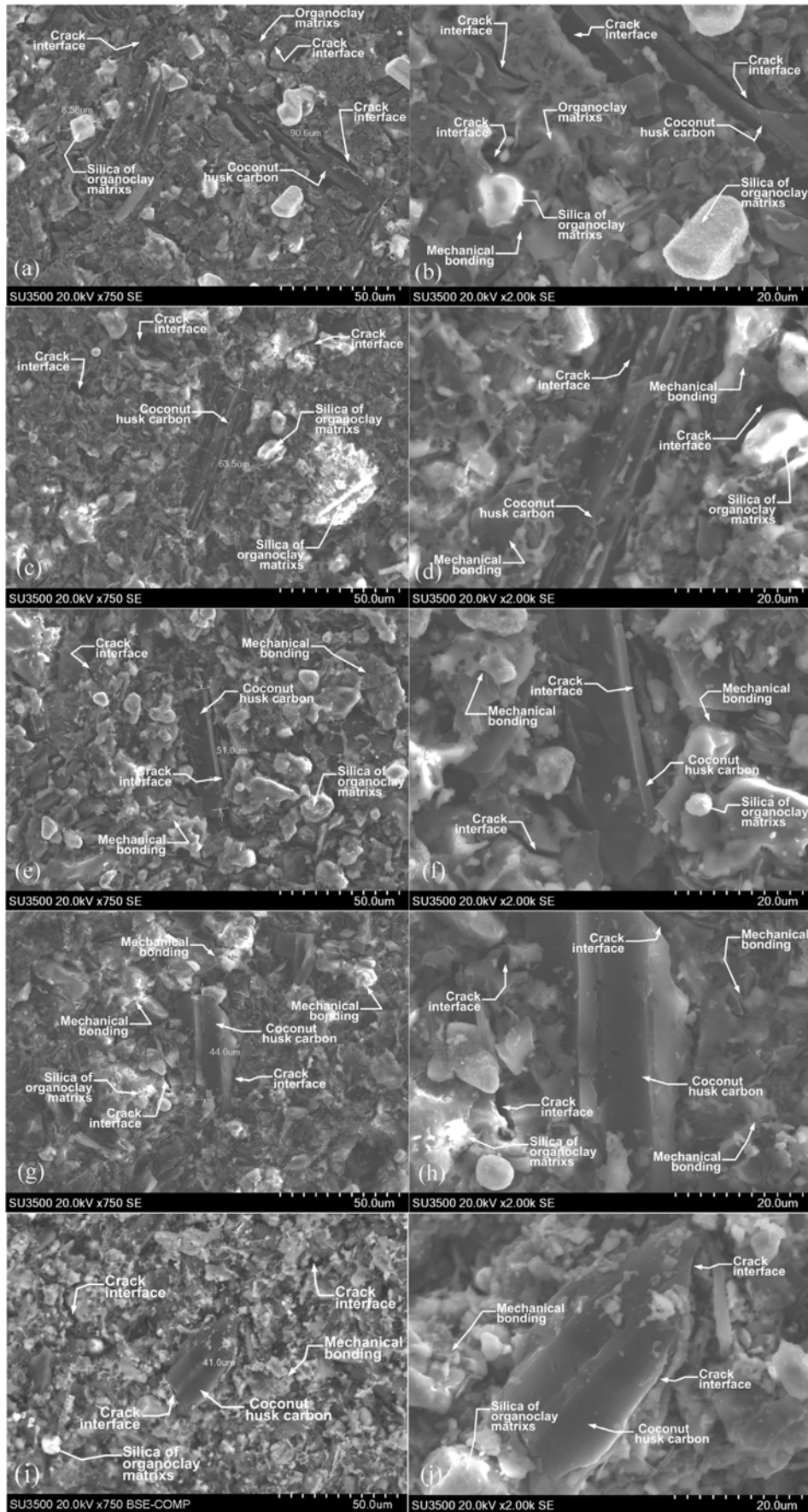


Fig. 14. Morphology of carbon-ceramic composite.

suspicion of porous and cracking is caused more by the irregular shape of carbon particles and matrix particles.

The cavities formed are also thought to be a result of the heating process in the sintering process, the particles forming the carbon-ceramic bonds have non-uniform volume expansion coefficients, resulting in pressing on each other and cracking even weaker particles mechanically. It is also suspected that bonding between particles is only mechanical in nature, relying only on the irregularity of the pairs of particles.

### Conclusion

At the carbon particle size of mesh #150; 200; 250, the electrical conductivity decreases, when the sintering temperature is raised, from 950 °C to 1050 °C. In mesh particle sizes # 300 and # 350, and higher sintering temperatures (from 950 °C - 1050 °C), this will increase electrical conductivity. The tendency of thermal conductivity follows the tendency of electrical conductivity, from the effect of carbon particle size. The higher the sintering temperature the higher the wear rate produced, this condition shows that the increase in sintering temperature tends to decrease the wear resistance properties, in other words, the softer the carbon-ceramic. Likewise, the smaller the particle size of carbon powder tends to increase the wear rate, meaning that carbon-ceramic is softer, and is not resistant to mechanical friction. The smaller the particle size of carbon, the density of carbon-ceramic composites that occur relatively no change. In general, the smaller the size of carbon particles in carbon-ceramic, the porosity of carbon-ceramic is relatively stable. There is no significant change. In fact, porosity tends to follow density, even though the size of carbon particles gets smaller. In general, an increase or decrease in density due to carbon particle size is followed by an increase or decrease in the electrical conductivity of carbon-ceramic. Compaction of 200 bar and with smaller particle size apparently can not eliminate porous or cracks that occur in the specimens. The occurrence of porous and cracking is more due to the irregular shape of carbon particles and matrix particles. Bonding between particles is only mechanical in nature, relying only on the irregularity of the pairs of particles.

### Acknowledgment

The DIPA of Politeknik Negeri Jakarta, Scheme of the Leading of Study Program Research has funded this study, Contract Number: 350 / PL3.18 / PN.00.03 / 2019, Fiscal Year 2019.

The author thanks P3M, Politeknik Negeri Jakarta.

### References

1. I. Štubňa, T. Húlan, T. Kaljuvee, and L. Vozár, *Appl. Clay*

2. Š. Csáki, J. Ondruška, V. Trnovcová, I. Štubňa, P. Dobroň, and L. Vozár, *Appl. Clay Sci.* 157 (2018) 19-23.
3. S. Ojha, S.K. Acharya, and G.J. Raghavendra, *Appl. Polym. Sci.* 132[1] (2015) 1-7.
4. M. Yates, M.A. Martín-luengo, L.V. Argomaniz, and S.N. Velasco, *Microporous Mesoporous Mater.* 154 (2012) 87-92.
5. A.E. Pramono, M.B.T. Firdaus, W. Ratriomasyo, M.Z. Nura, and J.W.M. Soedarsono, *J. Ceram. Process. Res.* 18[10] (2017) 748-753.
6. Y. Yao, B. Gao, J. Fang, M. Zhang, H. Chen, Y. Zhou, A. E. Creamer, Y. Sun, and L. Yang, *Chem. Eng. J.* 242 (2014) 136-143.
7. Y. He, L. Lu, S. Jin, and S. Hu, *Constr. Build. Mater.* 53 (2014) 131-137.
8. Z. Terzopoulou, D. Bikiaris, K.S. Triantafyllidis, G. Potsi, D. Gournis, G.Z. Papageorgiou, and P. Rudolf, *Thermochim. Acta* 642 (2016) 67-80.
9. T. Gumula, A. Rudawski, J. Michalowski, and S. Blazewicz, *Ceram. Int.* 41[6] (2015) 7381-7386.
10. M.S. Amin, S.M.A. El-gamal, and F.S. Hashem, *Constr. Build. Mater.* 98 (2015) 237-249.
11. R.L. Menchavez, M. Fujii, T. Shirai, and T. Kumazawa, *J. Eur. Ceram. Soc.* 34[3] (2014) 717-729.
12. C. Mauricio, R. Sanchez, S.N. Monteiro, N. Lalla, and N. Quaranta, *J. Mater. Res. Technol.* 2[2] (2013) 88-92.
13. B. Han, L. Zhang, C. Zhang, Y. Wang, X. Yu, and J. Ou, *Constr. Build. Mater.* 125 (2016) 479-489.
14. A. Wang, X. Gao, R.F.G. Jr, and D.D.L. Chung, *Carbon N. Y.* 59 (2013) 76-92.
15. A.E. Pramono, M. Zaki, J. Wahyuadi, M. Soedarsono, and N. Indayaningsih, *J. Ceram. Process. Res.* 20 (2019) 1-7.
16. A.E. Pramono, M.Z. Nura, J.W.M. Soedarsono, and N. Indayaningsih, *J. Ceram. Process. Res.* 20[4] (2019) 333-346.
17. V. Mymrin, C.F.G. Santos, K. Alekseev, M.A. Avanci, M.A. Kreuzsch, T. Borga, O. Graupmann, F.L. Cavalin, R.A. Monteiro, and V.A. Ruy Federal, *Appl. Clay Sci.* 155 (2018) 95-102.
18. F. Pardo, M.M. Jordan, and M.A. Montero, *Appl. Clay Sci.* 157 (2018) 158-164.
19. Z. Li, H. Zhang, P. Zhao, X. He, and X. Duan, *J. Korean Ceram. Soc.* 55[1] (2018) 36-43.
20. A. Mocciano, M.B. Lombardi, and A.N. Scian, *Appl. Clay Sci.* 153 (2018) 90-94.
21. F.O. Aramide and A.P. Popoola, *J. Ceram. Process. Res.* 19[2] (2018) 87-94.
22. N. Belmokhtar, H.E. Ayadi, M. Ammari, and L.B. Allal, *Appl. Clay Sci.* 162 (2018) 1-9.
23. A. Miras, E. Galán, I. González, A. Romero-Baena, and D. Martín, *Appl. Clay Sci.* 161 (2018) 176-183.
24. Y. He, L. Lu, S. Jin, and S. Hu, *Constr. Build. Mater.* 53 (2014) 131-137.
25. K.B. Choi, J.Y. Kim, S.M. Lee, K.H. Lee, and D.H. Yoon, *J. Korean Ceram. Soc.* 54[3] (2017) 257-260.
26. W. Sun, P. Zhang, K. Zhao, M. Tian, and Y. Wang, *Wear* 342-343 (2015) 172-180.
27. G. Zheng, J. Zhao, and Y. Zhou, *Wear* 290-291 (2012) 41-50.
28. L.M. Manocha, G. Prasad, and S. Manocha, *Mech. Adv. Mater. Struct.* 21[3] (2014) 172-180.
29. N.C. Kaushik and R.N. Rao, *Tribology Int.* 103 (2016) 298-308.
30. A.E. Pramono, *J. Mater. Sci. Eng. B* 3 (2013) 700-706.

31. D.S. Kim, J.S. Kim, and C.I. Cheon, *J. Korean Ceram. Soc.* 53[2], (2016) 162-166.
32. H.P.A. Alves, J.B. Silva, L.F.A. Campos, S.M. Torres, R.P.S. Dutra, and D.A. Macedo. *Ceram. Int.* 42[16] (2016) 19086-19090.
33. D.O. Obada, D. Dodoo-Arhin, M. Dauda, F.O. Anafi, A.S. Ahmed, and O.A. Ajayi, *Appl. Clay Sci.* 150 (2017) 175-183.
34. Z. Hongxia, D. Yongsheng, Y. Xiaowei, O. Shunli, and L. Baowei, *J. Ceram. Process. Res.* 18 (2017) 604-610.
35. C.H. Ting, S. Ramesha, C.Y. Tan, N.I. Zainal Abidin, W.D. Teng, I. Urriés, and L.T. Bang, *J. Ceram. Process. Res.* 18[8] (2017) 569-574.
36. J. Park, J.G. Yeo, S. Yang, and C.H. Cho, *J. Ceram. Process. Res.* 19 (2018) 20-24.
37. S.H. Mahdi, I.A. Hamad, and A.M. Ibraheim, *Mesopotamia Environ. J. Mesop.* 17 (2016) 10-17.
38. J. Ondruška, Š. Csáki, V. Trnovcová, I. Štubňa, F. Lukáč, J. Pokorný, L. Vozár, and P. Dobroň. *Appl. Clay Sci.* 154 (2018) 36-42.
39. S.N. Khosla, R.K. Bedi, and C.S. Gupta, *Trans. Indian Ceram. Soc.* ISSN 5456 (2014) 8-12.
40. J.-W. Lee, W.-J. Lee, and S.-M. Lee, *J. Korean Ceram. Soc.* 53[6] (2016) 635-640.
41. Y.K. Seo, Y.W. Kim, T. Nishimura, and W.S. Seo, *J. Eur. Ceram. Soc.* 36[15] (2016) 3755-3760.
42. Y.K. Seo, Y.W. Kim, K.J. Kim, and W.S. Seo, *J. Eur. Ceram. Soc.* 36[16] (2016) 3879-3887.
43. P.M. Nigay, T. Cutard, and A. Nzihou, *Ceram. Int.* 43[2] (2017) 1747-1754.
44. J. Bourret, A. Michot, N. Tessier-Doyen, B. Nait-Ali, F. Pennec, A. Alzina, J. Vicente, C.S. Peyratout, and D.S. Smith, *J. Am. Ceram. Soc.* 97[3] (2014) 938-944.
45. I. Allegretta, G. Eramo, D. Pinto, and A. Hein, *Appl. Clay Sci.* 135 (2017) 260-270.
46. I. Allegretta, G. Eramo, D. Pinto, and A. Hein, *Thermochim. Acta* 581 (2014) 100-109.
47. D. Buncianu, N. Tessier-Doyen, F. Courreges, and J. Absi, *Eur. J. Environ. Civ. Eng.* 21 (2017) 1270-1284.
48. L. Randazzo, G. Montana, A. Hein, A. Castiglia, G. Rodonò, and D.I. Donato, *Appl. Clay Sci.* 132-133 (2016) 498-507.
49. J. Bourret, N. Tessier-doyen, R. Guinebretiere, E. Joussein, and D.S. Smith, *Appl. Clay Sci.* 116-117 (2015) 150-157.
50. Y.P. Delgado, M.H. Staia, O. Malek, J. Vleugels, and P. De Baets, *Wear* 317[1-2] (2014) 104-110.
51. G. Byeong-Choon and C. In-Sik, *Materials (Basel)*. 10[7] (2017) 701.
52. Q.A. AL Rashid, H.M. Abuel-Naga, E.C. Leong, Y. Lu, and H. Al Abadi, *Appl. Clay Sci.* 156 (2018) 1-10.
53. Z. Chu, C. Jia, J. Liu, R. Ding, and G. Yuan, *J. Ceram. Sci. Technol.* 8[4] (2017) 499-504.
54. B.M. Bishui and J. Prasad, *Trans. Indian Ceram. Soc.* (2014) 109-115.